Comput. Mech. (2006) 38: 417–429
DOI 10.1007/s00466-006-0066-5

ORIGINAL PAPER

Ulrich Küttler · Christiane Förster · Wolfgang A. Wall

A solution for the incompressibility dilemma in partitioned fluid–structure interaction with pure Dirichlet fluid domains

Received: 31 January 2006 / Accepted : 15 February 2006 / Published online: 29 March 2006

Abstract In a subset of fluid–structure interaction (FSI) problems of incompressible flow and highly deformable structures all popular partitioned approaches fail to work. This also holds for recently quite popular strong coupling approaches based on Dirichlet–Neumann substructuring. This subset can be described as the special case where the fluid domain is entirely enclosed by Dirichlet boundary conditions, i.e. prescribed velocities. A vivid simple example would be a balloon with prescribed inflow rate. In such cases the incompressibility of the fluid cannot be satisfied during standard alternating FSI iterations as the deformation of the coupling surface is determined by the structural displacement that usually does not know about the current constraint on the fluid field. By analyzing this deficiency of the partitioned algorithm a small augmentation is proposed which allows to overcome the dilemma of incompressibility and fixed boundary velocities by introducing the volume constraint on the structural system of equations. In contrast to the original accelerated strong coupling partitioned method, the relaxation which ensures convergence of the iteration over the different fields has now to be performed on the coupling forces rather than on the displacements. In addition, two alternative approaches are discussed for the solution of the dilemma. The capability of the proposed method to deal with largely changing volumes of enclosed fluid is demonstrated by means of numerical examples.

Keywords Incompressible fluid · Fluid–structure interaction · Pure Dirichlet domain · Augmented Dirichlet–Neumann approach

U. Küttler · W. A. Wall (✉)
Chair of Computational Mechanics, TU Munich,
Boltzmannstr. 15, 85748
Garching, Germany
E-mail: wall@lnm.mw.tum.de

C. Förster
Institute of Structural Mechanics, University of Stuttgart
Pfaffenwaldring 7, 70550 Stuttgart, Germany

1 Introduction

Due to the wide application area in many engineering fields and applied sciences fluid–structure interaction (FSI) of incompressible flows and flexible structures is a persistent matter of interest.

Partitioned coupling approaches are an appreciated tool for solving FSI problems. In particular, the so-called Dirichlet–Neumann algorithm where the fluid serves as Dirichlet partition inheriting displacement (velocity) boundary conditions from the structure while the structure, i.e. the Neumann partition, is loaded by the fluid pressure (and viscous stresses) has shown to be robust and efficient [6, 7, 10, 14, 17, 21–24, 26]. We consider an implementation where an arbitrary Lagrangian–Eulerian (ALE) formulation is employed in order to account for the temporal deformation of the fluid domain $\Omega^{\mathrm{F}}(t)$. Thus, the fluid mesh is adjusted to the structural deformation prior to the solution of the flow equations. However, most of the issues discussed in this paper also hold for other Dirichlet–Neumann approaches for FSI, e.g. those based on fixed grid schemes.

Unfortunately, these algorithms fail completely as soon as the fluid is entirely enclosed by Dirichlet type of boundaries. This situation occurs when a structure is to be filled by a prescribed flow rate, i.e. in a balloon type of problem. Besides classical balloon problems such situations appear, e.g. in flexible tube systems where velocity profiles are given and prescribed at certain cross sections or in the coupled biomechanical analysis of the respiratory system. However, weakened versions of the prescribed dilemma, also causing numerical problems, might appear when quasi-enclosed fluid regions occur in complex situations and geometries.

Prescribing the inflow and outflow velocities on all boundaries while the volume of the entire fluid domain is determined from the structural displacement yields an ill-posed problem on the fluid domain and hence failure of the overall algorithm. A close look reveals that the difficulty consists of two parts. Firstly, an incompressible flow has to be solved on an appropriately sized domain: the volume constraint of the fluid volume has to be considered within the solution of

the structural equations. A second question arises when the absolute pressure level inside the fluid has to be determined. While the fluid pressure in most applications is adjusted to the external pressure at a Neumann boundary Γ_N of the fluid field the pressure inside an enclosed fluid is determined indirectly by the external pressure on the deforming structural parts.

An augmentation of the classical Dirichlet–Neumann algorithm is proposed which allows to obtain the fluid pressure level such that the structural response satisfies the volume constraint. To reach this the structural equations are enriched by the volume condition where the corresponding Lagrange multiplier provides the unknown pressure level information.

Partitioned block Gauß–Seidel FSI algorithms require some amount of relaxation to ensure and accelerate convergence [2, 8, 16, 17, 26]. The traditional relaxation of the structural displacements at the coupling interface Γ_{FSI} can, however, not be employed on the modified algorithm where the displacements have been determined with the side condition of the constrained fluid volume. Otherwise the constraint would again be violated. Thus, in our case the relaxation has to be done on the force coupling information in order to preserve the algorithms' robustness.

In addition, two alternative approaches to tackle the pure Dirichlet fluid dilemma in FSI are also discussed briefly. In the first case, the problem is tried to be avoided through an engineering-wise counterintuitive algorithm, where the fields within the partitioned algorithm are exchanged such that the structure exerts forces upon the fluid field which reacts by interface displacements, i.e. using a Neumann–Dirichlet algorithm. While relaxing the Dirichlet boundary problem and passing the force information from the structure to the fluid in a natural way this approach faces new challenges as a free surface like formulation is required on the fluid side. Additionally, the resulting algorithm is numerically highly sensitive if reasonable material parameters are applied. It also fails for fully embedded incompressible structures. A second alternative was presented in [19]. Here the artificial compressibility approach introduces the need for additional iterations and thus highly increases the required numerical effort. In addition, this approach lacks robustness for general complex cases.

After introducing the governing equations in Sect. 2 the partitioned Dirichlet–Neumann algorithm is briefly reviewed in Sect. 3. In Sect. 4 the difficulties in the case of fully Dirichlet enclosed fluid domains are discussed. An augmentation to the algorithm that allows to solve FSI problems with pure Dirichlet constrained fluid partitions in a partitioned manner is presented in Sect. 5. In Sect. 6 alternative strategies are reviewed. Numerical results obtained by means of the developed algorithm are presented in Sect. 7.

2 Governing equations

2.1 Structural domain

Within the considered FSI problems large structural deformations are expected. Thus, geometrical nonlinearities have to be taken in to account. Linear material response is assumed for simplicity while the formulation can easily be extended to more general material laws as can be seen in the examples in Sect 7. The structural displacements $\mathbf{d}$ are governed by the geometrically nonlinear elastodynamics equations

$$\rho^S \frac{D^2\mathbf{d}}{Dt^2} = \nabla \cdot \mathbf{S} + \rho^S \mathbf{f}^S \qquad \text{in } \Omega^S \times (0,T), \tag{1}$$

where ρ^S and $\mathbf{f}^S$ represent the structural density and specific body force, respectively. The differential D denotes the material time derivative. For the structural equations, a Lagrangian formulation will be used throughout this paper. The second Piola–Kirchhoff stress tensor $\mathbf{S}$ is related to the Green–Lagrangian strains via

$$\mathbf{S} = \mathbf{C} : \mathbf{E} \quad \text{with} \quad \mathbf{E} = \frac{1}{2}\left(\mathbf{F}^T \cdot \mathbf{F} - \mathbf{I}\right), \tag{2}$$

where $\mathbf{C}$ denotes the material tensor and $\mathbf{F} = \nabla\mathbf{d}$ represents the deformation gradient. The time-dependent problem (1) is subject to the initial and boundary conditions

$$\mathbf{d} = \mathbf{d}_0 \quad \text{and} \quad \dot{\mathbf{d}} = \dot{\mathbf{d}}_0 \quad \text{in } \Omega^S \text{ at } t = 0 \tag{3}$$

$$\mathbf{d} = \hat{\mathbf{d}} \quad \text{on } \Gamma_D^S, \qquad \mathbf{S}\cdot\mathbf{n} = \hat{\mathbf{h}}^S \quad \text{on } \Gamma_N^S, \tag{4}$$

where Γ_D^S and Γ_N^S denote the Dirichlet and Neumann partition of the structural boundary, respectively, and $\hat{\mathbf{d}}$ and $\hat{\mathbf{h}}^S$ denote the prescribed Dirichlet and Neumann values.

Using finite elements the semidiscrete structural equations read

$$\mathbf{M}^S\ddot{\mathbf{d}} + \mathbf{N}^S(\mathbf{d}) = \mathbf{f}^S, \tag{5}$$

where $\mathbf{M}^S$ represents the structural mass matrix while $\mathbf{N}^S$ and $\mathbf{f}^S$ denote the internal and external forces, respectively. The nodal displacement vector is given by $\mathbf{d}$ while the overset dot represents the respective time derivatives, i.e. accelerations. In the present approach, this system is solved using the nonlinear version of the 'generalized-α method' of Chung and Hulbert [4] along with consistent linearization and a Newton–Raphson iterative scheme.

2.2 Fluid domain

The fluid under consideration is assumed Newtonian and its motion is governed by the incompressible Navier–Stokes equations. The flow equations that determine the flow velocities $\mathbf{u}$ and pressure p read

$$\left.\frac{\partial\mathbf{u}}{\partial t}\right|_\chi + \left(\mathbf{u} - \mathbf{u}^G\right)\cdot\nabla\mathbf{u} - 2\nu\nabla\cdot\boldsymbol{\varepsilon}(\mathbf{u}) + \nabla p = \mathbf{f}^F \quad \text{in } \Omega^F \times (0,T), \tag{6}$$

$$\nabla\cdot\mathbf{u} = 0 \quad \text{in } \Omega^F \times (0,T). \tag{7}$$

with the grid velocity $\mathbf{u}^G$. The parameter $\nu = \mu/\rho^F$ denotes the kinematic viscosity where μ represents the viscosity and ρ^F the density of the fluid. The vector field $\mathbf{f}^F$ denotes the specific body force on the fluid. The kinematic pressure is represented by p where $\bar{p} = p\,\rho^F$ is the physical pressure within the fluid field.

The balance of linear momentum (6) refers to a deforming ALE frame of reference denoted by $\boldsymbol{\chi}$ where the geometrical location of a mesh point is obtained from the unique mapping $\mathbf{x} = \varphi(\boldsymbol{\chi}, t)$.

The stress tensor of a Newtonian fluid is given by

$$\boldsymbol{\sigma}^{\mathrm{F}} = -\bar{p}\,\mathbf{I} + 2\mu\boldsymbol{\varepsilon}(\mathbf{u}) \quad \text{where} \quad \boldsymbol{\varepsilon}(\mathbf{u}) = \frac{1}{2}\left(\nabla\mathbf{u} + \nabla\mathbf{u}^{\mathrm{T}}\right) \tag{8}$$

denotes the strain rate tensor.

The partial differential equations (6) are subject to initial and boundary conditions

$$\begin{aligned} &\mathbf{u} = \mathbf{u}_0 \quad \text{in } \Omega^{\mathrm{F}} \text{ at } t = 0 \\ &\mathbf{u} = \hat{\mathbf{u}} \quad \text{on } \Gamma^{\mathrm{F}}_{\mathrm{D}}, \qquad \boldsymbol{\sigma}\cdot\mathbf{n} = \hat{\mathbf{h}}^{\mathrm{F}} \quad \text{on } \Gamma^{\mathrm{F}}_{\mathrm{N}}, \end{aligned} \tag{9}$$

where the present study is concerned with cases where no Neumann portion of the fluid boundary is present i.e. $\partial\Omega^{\mathrm{F}} = \Gamma^{\mathrm{F}}_{\mathrm{D}}$.

Equation (6) discretized by finite elements in space yields the matrix representation

$$\mathbf{M}^{\mathrm{F}}\dot{\mathbf{u}} + \mathbf{N}^{\mathrm{F}}(\mathbf{u})\mathbf{u} + \mathbf{K}^{\mathrm{F}}\mathbf{u} + \mathbf{G}^{\mathrm{F}}\mathbf{p} = \mathbf{f}^{\mathrm{F}}, \qquad \left(\mathbf{G}^{\mathrm{F}}\right)^{\mathrm{T}}\mathbf{u} = \mathbf{0}, \tag{10}$$

where $\mathbf{M}^{\mathrm{F}}$ represents the fluid mass matrix, $\mathbf{N}^{\mathrm{F}}(\mathbf{u})$ and $\mathbf{K}^{\mathrm{F}}$ denote the nonlinear convective and viscous matrix, respectively, and $\mathbf{f}^{\mathrm{F}}$ is the vector of nodal body forces. The matrix $\mathbf{G}^{\mathrm{F}}$ represents the discrete gradient operator. The details of a correct discretization of the ALE formulation of the Navier–Stokes equations by means of stabilized finite elements are given in [9].

Implicit one-step-θ and BDF2 schemes are used to discretize Eq. (10) in time. The occurring nonlinearities are dealt with using Newton or fixed-point-like iteration schemes [25].

3 Partitioned solution of the FSI problem

Equations (5) and (10) together with an appropriate mesh moving algorithm form a highly nonlinear coupled system of equations. To solve it several strategies can be pursued, ranging from fully coupled monolithic approaches [12, 13] to weakly coupled staggered schemes [18]. In between these there are iterative or strong coupling schemes [7, 11, 14, 15, 17, 21, 23, 26] that are particularly favorable in many cases. Just as the monolithic schemes the iteratively coupled ones converge to the exact solution and still the individual fields are solved independently of each other. In the following only partitioned solution approaches are considered.

3.1 Partitioned solution approach

The nature of the FSI problem suggests a nonoverlapping domain decomposition with fluid field and structure field acting as separate domains. The wet structural surface acts as the coupling interface Γ_{FSI} for brevity being denoted as Γ in the following.

Key requirement for the coupling schemes is to fulfill the discrete version of the kinematic and the dynamic continuity across the interface at all discrete time levels.

$$\mathbf{d}_\Gamma(t)\cdot\mathbf{n} = \mathbf{r}_\Gamma(t)\cdot\mathbf{n} \quad \text{and}$$

$$\mathbf{u}_\Gamma(t)\cdot\mathbf{n} = \mathbf{u}^{\mathrm{G}}_\Gamma(t)\cdot\mathbf{n} = \left.\frac{\partial\mathbf{r}_\Gamma(t)}{\partial t}\right|_{\boldsymbol{\chi}}\cdot\mathbf{n} \tag{11}$$

$$\boldsymbol{\sigma}^{\mathrm{S}}_\Gamma(t)\cdot\mathbf{n} = \boldsymbol{\sigma}^{\mathrm{F}}_\Gamma(t)\cdot\mathbf{n} \tag{12}$$

with $\mathbf{r}$ denoting the fluid mesh displacements and $\mathbf{n}$ the unit normal vector on the interface. Satisfying the kinematic continuity leads to mass conservation at Γ_{FSI}, satisfying the dynamic continuity yields conservation of linear momentum, and energy conservation finally requires to simultaneously satisfy both continuity equations.

The algorithmic framework of the partitioned FSI analysis is discussed in detail in [5, 16].

3.2 Nonoverlapping Dirichlet–Neumann partitioning

The Dirichlet–Neumann partitioning with the fluid domain acting as Dirichlet partition with prescribed velocities $\mathbf{u}_\Gamma$ and the structure domain acting as Neumann partition loaded with interface forces $\mathbf{f}_\Gamma$ is particularly suited for partitioned FSI solutions.

A Dirichlet–Neumann coupling algorithm with synchronous time discretization and block Gauß–Seidel iteration using Aitken-style relaxation is considered here. This formulation has shown to be efficient [16, 17, 26] and it provides the framework that we will subsequently enhance to work for temporally changing fully Dirichlet constraint fluid domains also. The same reasoning can be applied to Newton–Raphson based field iteration schemes, though.

In the following $(\cdot)_{\mathrm{I}}$ and $(\cdot)_\Gamma$ denote variables or coefficients in the interior of a subdomain Ω^j and on the coupling interface, respectively, while a vector without any of the subscripts I and Γ comprises degrees of freedom on the entire subdomain including interior and interface.

To highlight the coupling behavior the following outline abbreviates the nonlinear field equations (5) and (10) with the symbolic systems

$$\mathbf{A}^{\mathrm{S}}\mathbf{d}^{\mathrm{S}} = \mathbf{f}^{\mathrm{S}} \quad \text{and} \quad \mathbf{A}^{\mathrm{F}}\mathbf{u}^{\mathrm{F}} = \mathbf{f}^{\mathrm{F}} \tag{13}$$

for the structure field and the fluid field, respectively.

In every time step the subsequent calculations have to be performed.

1. Transfer the latest structure displacements $\mathbf{d}^{\mathrm{S}}_{\Gamma,i+1}$ to the fluid field, determine the appropriate fluid velocities at the interface $\mathbf{u}^{\mathrm{S}}_{\Gamma,i+1}$ from the structure displacements and calculate the fluid domain deformation.
2. Solve for the inner fluid velocities and pressures $\mathbf{u}^{\mathrm{F}}_{\mathrm{I},i+1}$
$$\mathbf{A}^{\mathrm{F}}_{\mathrm{II}}\mathbf{u}^{\mathrm{F}}_{\mathrm{I},i+1} = \mathbf{f}^{\mathrm{F}}_{\mathrm{I}\,\mathrm{ext}} - \mathbf{A}^{\mathrm{F}}_{\mathrm{I}\Gamma}\mathbf{u}^{\mathrm{S}}_{\Gamma,i+1} \tag{14}$$
3. Find the fluid forces at the interface Γ_{FSI}
$$\mathbf{f}^{\mathrm{F}}_{\Gamma,i+1} = \mathbf{A}^{\mathrm{F}}_{\Gamma\mathrm{I}}\mathbf{u}^{\mathrm{F}}_{\mathrm{I},i+1} + \mathbf{A}^{\mathrm{F}}_{\Gamma\Gamma}\mathbf{u}^{\mathrm{S}}_{\Gamma,i+1} \tag{15}$$

4. Solve for the structural displacements

$$\begin{bmatrix} \mathbf{A}^{\mathrm{S}}_{\Gamma\Gamma} & \mathbf{A}^{\mathrm{S}}_{\Gamma\mathrm{I}} \\ \mathbf{A}^{\mathrm{S}}_{\mathrm{I}\Gamma} & \mathbf{A}^{\mathrm{S}}_{\mathrm{II}} \end{bmatrix} \begin{bmatrix} \tilde{\mathbf{d}}^{\mathrm{S}}_{\Gamma,i+1} \\ \mathbf{d}^{\mathrm{S}}_{\mathrm{I},i+1} \end{bmatrix} = \begin{bmatrix} \mathbf{f}^{\mathrm{S}}_{\Gamma\,\mathrm{ext}} - \mathbf{f}^{\mathrm{F}}_{\Gamma,i} \\ \mathbf{f}^{\mathrm{S}}_{\mathrm{I}\,\mathrm{ext}} \end{bmatrix} \tag{16}$$

5. Relax the interface displacement

$$\mathbf{d}^{\mathrm{S}}_{\Gamma,i+1} = \omega_i \tilde{\mathbf{d}}^{\mathrm{S}}_{\Gamma,i+1} + (1-\omega_i)\mathbf{d}^{\mathrm{S}}_{\Gamma,i} \tag{17}$$

The iteration finishes when the error of the interface displacement $\tilde{\mathbf{d}}^{\mathrm{S}}_{\Gamma,i+1}$ is sufficiently small.

4 Dilemma with fully enclosed, i.e. Dirichlet-constraint, fluid domains

The Dirichlet–Neumann algorithm described above fails if there are prescribed velocities on all boundaries of the fluid domain. A fully Dirichlet-bounded fluid domain can only be solved if (1) the prescribed velocities satisfy the mass balance of the incompressible fluid and (2) the pressure level is fixed by an additional constraint. Standard Dirichlet–Neumann algorithms fail on both conditions.

4.1 Interface velocity $\mathbf{u}_\Gamma$ constraint

Concerning the boundary velocities the incompressibility constraint on a deforming domain translates to

$$\Delta V^n = V^{n+1} - V^n = \int_{\Delta t}\int_{\Gamma^{\mathrm{F}}} \mathbf{u}\cdot\mathbf{n}\,\mathrm{d}\Gamma\,\mathrm{d}t \tag{18}$$

where Γ^{F} represents the boundary of the fluid domain and V^{n+1} and V^n denote the volume of the enclosed fluid domain at the discrete time steps t^{n+1} and t^n, respectively.

The fluid domain boundary Γ^{F} consists of inflow and outflow regions, rigid walls, and the coupling interface.

$$\Gamma^{\mathrm{F}} := \Gamma_{\mathrm{in}} \cup \Gamma_{\mathrm{out}} \cup \Gamma_{\mathrm{wall}} \cup \Gamma_{\mathrm{FSI}} \tag{19}$$

The volume change ΔV^n in one time step depends on inflow and outflow, thus condition (18) constrains the interface velocity $\mathbf{u}_\Gamma$ at the coupling interface Γ_{FSI}. In the Dirichlet–Neumann coupling it is the structural solution that determines the interface displacements $\mathbf{d}_\Gamma$ and thus the interface velocities $\mathbf{u}_\Gamma$. Physically the fluid's incompressibility constrains the admissible structure solutions while within standard partitioned algorithms this constraint is not known by the structure.

Consequently within the Dirichlet–Neumann algorithm the first attempt of a fluid solution on a not yet converged domain will create an ill-posed problem yielding to the failure of the overall formulation.

4.2 Pressure level determination

The pressure level of a fluid domain with prescribed velocities on all boundaries is undetermined as the pressure is defined in Eq. (6) up to a constant. Thus, the pressure level has to be specified by an additional constraint.

A coupled FSI system does specify the pressure level of the fluid domain even if both inflow and outflow velocities are prescribed. The pressure of the fluid is most intimate related to the stresses of the structure at the interface according to the equilibrium coupling condition (12). That condition holds by design in a Dirichlet–Neumann algorithm, however because the fluid mass balance constrains the admissible structure deformations the fluid pressure must be such that the resulting structure deformation matches the fluid volume change. That is the structure has to prescribe the pressure level of the fluid. Without modification the Dirichlet–Neumann algorithm does not provide the required exchange of pressure information.

4.2.1 Simple illustratory example

This situation can be easily illustrated in an incompressible version of the piston problem (see Fig. 1). If the mass–spring system does not know about the inflow into the fluid region within a time step, it cannot deform accordingly and the next fluid solution will immediately fail. This will happen no matter whether standard staggered or iterative coupling schemes are used.

It could be argued that in this simple case the structural deformation is defined only by the inflow velocity and consequently the pressure level in the fluid is defined by the spring force resulting from this deformation.

4.3 Remedies

Above two difficulties are closely related. The two fields are coupled much closer as compared to FSI problems with free outflow boundaries. Therefore, any attempt to overcome the difficulties will result in an algorithm that is more expensive from a numerical point of view.

Several strategies might be pursued to arrive at a working coupling algorithm. The ones considered here are:

- The fluids' mass balance constraint on the interface displacements has to be satisfied by the structure. Thus, the introduction of a constraint in the structure equation avoids incompressibility violations in the Dirichlet–Neumann algorithm. The pressure level coupling needs additional considerations. This approach is presented in detail in Sect. 5.
- Another point of departure is the pressure level coupling between structure and fluid. The natural way for the structure to determine the fluid pressure is to transfer interface forces from the structure to the fluid. It follows that the fluid has to prescribe the interface displacements on the structure, that is the Dirichlet–Neumann coupling is reversed to a Neumann–Dirichlet approach. This is considered in Sect. 6.1.
- Finally, the whole problem is avoided if one can get rid of the incompressibility constraint, at least temporarily. Some remarks on this idea follow in Sect. 6.2.

Fig. 1 The simple piston problem with incompressible fluid raises the dilemma for standard coupling algorithms

It is worth noting, that according to the insight discussed so far Dirichlet–Neumann approaches only work in standard examples because the fluid can temporarily escape through the Neumann boundary in staggered situations or during the field iterations in strong coupling schemes.

5 Volume constraint applied to the structural equation: augmented Dirichlet–Neumann approach

Above discussion and insight directly points to possible solutions of the dilemma. In this respect a consequent approach which exchanges more information between structure field and fluid field is to introduce the volume constraint into the structural equation. The temporal evolution of the enclosed volume is determined by the Dirichlet boundary conditions of the fluid domain. With the prescribed volume at the new time step V_c a temporally discretized version of Eq. (18) amounts to

$$\begin{aligned} V_c = V^{n+1} &= V^n + \int_{\Gamma^F} \frac{1}{2}\Delta t \left(\mathbf{u}^{n+1}\cdot\mathbf{n} + \mathbf{u}^n\cdot\mathbf{n}\right) \mathrm{d}\Gamma \\ &= V^n + \int_{\Gamma_{FSI}} \left(\mathbf{r}^{n+1}\cdot\mathbf{n} - \mathbf{r}^n\cdot\mathbf{n}\right) \mathrm{d}\Gamma \\ &\quad + \int_{\Gamma_{in}\cup\Gamma_{out}} \frac{1}{2}\Delta t \left(\mathbf{u}^{n+1}\cdot\mathbf{n} + \mathbf{u}^n\cdot\mathbf{n}\right) \mathrm{d}\Gamma \end{aligned} \tag{20}$$

where $\mathbf{r}^{n+1}$ and $\mathbf{r}^n$ are the interface positions at the time t^{n+1} and t^n. The constraint $V_c - V = 0$ is introduced into the structural equation of motion by means of a Lagrange multiplier yielding the weak form

$$\begin{aligned} &\left(\varrho\ddot{\mathbf{d}}, \delta\mathbf{d}\right) + (\delta\mathbf{E}, \mathbf{S}) - \left(\lambda, \frac{\mathrm{d}V}{\mathrm{d}\mathbf{d}}\delta\mathbf{d}\right)_{\Gamma_{FSI}} \\ &= (\varrho\mathbf{b}, \delta\mathbf{d}) + \left(\hat{\mathbf{t}}, \delta\mathbf{d}\right)_{\Gamma_N} + \left(\mathbf{f}^F, \delta\mathbf{d}\right)_{\Gamma_{FSI}} \\ &\quad (\delta\lambda, V_c - V(\mathbf{d}))_{\Gamma_{FSI}} = 0 \end{aligned} \tag{21}$$

where the Lagrange multiplier λ represents the physical pressure level required to satisfy the volume constraint on the structure. The forces $\mathbf{f}^F$ at the interface Γ_{FSI} are the coupling forces from the fluid.

If the fluid forces at the interface $\mathbf{f}^F$ are sufficient to maintain the required volume V_c, the additional pressure λ will be zero. This can be achieved by a coupling algorithm that transfers λ to the fluid partition and adds it to the pressure boundary condition which is used to determine the pressure level. This way the additional pressure λ will tend to zero in the course of the coupling iteration.

But changing pressure boundary condition during the coupling iteration raises issues with the relaxation. It is generally advisable to avoid it. Instead the fluid pressure level can be fixed to a constant value in the fluid domain. Of course the resulting additional pressure λ will not vanish in this case. It is added to the fluid pressure values $\overline{p}^F$ after the fluid calculation to obtain the final pressure $\overline{p}$.

$$\overline{p} = \overline{p}^F + \lambda \tag{22}$$

This approach is followed in the examples presented in Sect. 7.

5.1 Calculation of the enclosed fluid volume

The solution of the constrained structure equation (21) by a Newton–Raphson iteration demands the calculation of the enclosed fluid volume and the linearization thereof. The volume of a fully enclosed region can be given by integrating the height function z over the surface Γ^F.

$$V = \oint_{\Gamma^F} z(x, y)\, \mathrm{d}\Gamma \tag{23}$$

Thus, a simple way to determine the enclosed volume in a discretized setting is to sum the volumes between the surfaces of the boundary elements and the x, y plane.

$$V = \sum_{el} \int_{\Gamma^F} z(x, y)\, \mathrm{d}\Gamma \tag{24}$$

This equation is valid as long as the whole fluid boundary is taken into account and the element nodes are enumerated in a positive manner. From this expression it is straightforward to evaluate the derivatives of the volume with respect to the node positions.

5.2 Modified Dirichlet–Neumann coupling with volume constraint

The iterative coupling algorithm with the volume constraint in the structural equation is a slight modification of the algorithm in Sect. 3.2. Because the structure solver has to account for the volume condition of the fluid domain, the displacement of the interface cannot be altered once the structure solution is done. In particular, the relaxation of the displacements is no longer possible. Instead, because relaxation is needed to enforce and accelerate convergence, one has to relax the fluid forces at the interface.

By means of the symbolic structural and fluid system (13) in every time step the following calculations have to be performed.

1. Solve for the structure displacements loaded with the fluid forces $\mathbf{f}^F_{\Gamma,i}$, but respect the volume constraint required by

the fluid (20)

$$\begin{bmatrix} \mathbf{A}^{\mathrm{S}}_{\Gamma\Gamma} & \mathbf{A}^{\mathrm{S}}_{\Gamma\mathrm{I}} & -V_{,\mathbf{d}^{\mathrm{S}}_{\Gamma}} \\ \mathbf{A}^{\mathrm{S}}_{\mathrm{I}\Gamma} & \mathbf{A}^{\mathrm{S}}_{\mathrm{II}} & 0 \\ -V_{,\mathbf{d}^{\mathrm{S}}_{\Gamma}} & 0 & 0 \end{bmatrix} \begin{bmatrix} \mathbf{d}^{\mathrm{S}}_{\Gamma,i+1} \\ \mathbf{d}^{\mathrm{S}}_{\mathrm{I},i+1} \\ \lambda_{i+1} \end{bmatrix} = \begin{bmatrix} \mathbf{f}^{\mathrm{S}}_{\Gamma\,\mathrm{ext}} - \mathbf{f}^{\mathrm{F}}_{\Gamma,i} - V_{,\mathbf{d}^{\mathrm{S}}_{\Gamma}}\lambda_i \\ \mathbf{f}^{\mathrm{S}}_{\mathrm{I}\,\mathrm{ext}} \\ V_{\mathrm{c}} - V_{,\mathbf{d}^{\mathrm{S}}_{\Gamma}}\mathbf{d}^{\mathrm{S}}_{\Gamma,i} \end{bmatrix} \tag{25}$$

2. Transfer the interface displacements $\mathbf{d}^{\mathrm{S}}_{\Gamma,i+1}$ to the fluid and determine the interface velocities $\mathbf{u}^{\mathrm{S}}_{\Gamma,i+1}$. Solve for the inner fluid velocities and pressures $\mathbf{u}^{\mathrm{F}}_{\mathrm{I},i+1}$

$$\mathbf{A}^{\mathrm{F}}_{\mathrm{II}}\mathbf{u}^{\mathrm{F}}_{\mathrm{I},i+1} = \mathbf{f}^{\mathrm{F}}_{\mathrm{I}\,\mathrm{ext}} - \mathbf{A}^{\mathrm{F}}_{\mathrm{I}\Gamma}\mathbf{u}^{\mathrm{S}}_{\Gamma,i+1} \tag{26}$$

3. Find the fluid forces at the interface Γ_{FSI}

$$\tilde{\mathbf{f}}^{\mathrm{F}}_{\Gamma,i+1} = \mathbf{A}^{\mathrm{F}}_{\Gamma\mathrm{I}}\mathbf{u}^{\mathrm{F}}_{\mathrm{I},i+1} + \mathbf{A}^{\mathrm{F}}_{\Gamma\Gamma}\mathbf{u}^{\mathrm{S}}_{\Gamma,i+1} \tag{27}$$

4. Relax the fluid forces

$$\mathbf{f}^{\mathrm{F}}_{\Gamma,i+1} = \omega_i\tilde{\mathbf{f}}^{\mathrm{F}}_{\Gamma,i+1} + (1-\omega_i)\mathbf{f}^{\mathrm{F}}_{\Gamma,i} \tag{28}$$

The relaxation parameter ω_i can be calculated by any of the methods suggested in [16, 17].

The iteration finishes when the error of the fluid boundary force $\tilde{\mathbf{f}}^{\mathrm{F}}_{\Gamma,i+1}$ is sufficiently small.

5.3 Relaxation of coupling forces

The Dirichlet–Neumann coupling algorithm can be viewed as fixed point iteration for the interface displacements as shown by Mok [16] and accordingly relaxation of the interface displacements is needed. In the same way, however, the algorithm can be viewed as a fixed point iteration for the coupling forces. In this case, the forces at the interface amount to

$$\begin{aligned}\tilde{\mathbf{f}}^{\mathrm{F}}_{\Gamma,i+1} &= \mathbf{A}^{\mathrm{F}}_{\Gamma\mathrm{I}}\left(\mathbf{A}^{\mathrm{F}}_{\mathrm{II}}\right)^{-1}\left(\mathbf{f}^{\mathrm{F}}_{\mathrm{I}\,\mathrm{ext}} - \mathbf{A}^{\mathrm{F}}_{\mathrm{I}\Gamma}\mathbf{u}^{\mathrm{S}}_{\Gamma,i+1}\right) + \mathbf{A}^{\mathrm{F}}_{\Gamma\Gamma}\mathbf{u}^{\mathrm{S}}_{\Gamma,i+1} \\ &= \mathbf{A}^{\mathrm{F}}_{\Gamma\mathrm{I}}\left(\mathbf{A}^{\mathrm{F}}_{\mathrm{II}}\right)^{-1}\mathbf{f}^{\mathrm{F}}_{\mathrm{I}\,\mathrm{ext}} + \mathbf{S}^{\mathrm{F}}\mathbf{u}^{\mathrm{S}}_{\Gamma,i+1}\end{aligned} \tag{29}$$

with the Schur complement $\mathbf{S} = \mathbf{A}_{\Gamma\Gamma} - \mathbf{A}_{\Gamma\mathrm{I}}\mathbf{A}^{-1}_{\mathrm{II}}\mathbf{A}_{\mathrm{I}\Gamma}$. Ignoring the difference between displacements and velocities at the interface for the time being, that is ignoring the factor introduced by the time discretization, the structure displacements at the interface

$$\begin{aligned}\mathbf{d}^{\mathrm{S}}_{\Gamma,i+1} &= \left(\mathbf{A}^{\mathrm{S}}_{\Gamma\Gamma} - \mathbf{A}^{\mathrm{S}}_{\Gamma\mathrm{I}}\left(\mathbf{A}^{\mathrm{S}}_{\mathrm{II}}\right)^{-1}\mathbf{A}^{\mathrm{S}}_{\mathrm{I}\Gamma}\right)^{-1} \\ &\quad\times\left(\mathbf{f}^{\mathrm{S}}_{\Gamma\,\mathrm{ext}} - \mathbf{f}^{\mathrm{F}}_{\Gamma,i} - \mathbf{A}^{\mathrm{S}}_{\Gamma\mathrm{I}}\left(\mathbf{A}^{\mathrm{S}}_{\mathrm{II}}\right)^{-1}\mathbf{f}^{\mathrm{S}}_{\mathrm{I}\,\mathrm{ext}}\right) \\ &= \left(\mathbf{S}^{\mathrm{S}}\right)^{-1}\left(\mathbf{f}^{\mathrm{S}}_{\Gamma\,\mathrm{ext}} - \mathbf{f}^{\mathrm{F}}_{\Gamma,i} - \mathbf{A}^{\mathrm{S}}_{\Gamma\mathrm{I}}\left(\mathbf{A}^{\mathrm{S}}_{\mathrm{II}}\right)^{-1}\mathbf{f}^{\mathrm{S}}_{\mathrm{I}\,\mathrm{ext}}\right)\end{aligned} \tag{30}$$

can be substituted in Eq. (29)

$$\begin{aligned}\tilde{\mathbf{f}}^{\mathrm{F}}_{\Gamma,i+1} &= \mathbf{A}^{\mathrm{F}}_{\Gamma\mathrm{I}}\left(\mathbf{A}^{\mathrm{F}}_{\mathrm{II}}\right)^{-1}\mathbf{f}^{\mathrm{F}}_{\mathrm{I}\,\mathrm{ext}} + \mathbf{S}^{\mathrm{F}}\left(\mathbf{S}^{\mathrm{S}}\right)^{-1} \\ &\quad\times\left(\mathbf{f}^{\mathrm{S}}_{\Gamma\,\mathrm{ext}} - \mathbf{f}^{\mathrm{F}}_{\Gamma,i} - \mathbf{A}^{\mathrm{S}}_{\Gamma\mathrm{I}}\left(\mathbf{A}^{\mathrm{S}}_{\mathrm{II}}\right)^{-1}\mathbf{f}^{\mathrm{S}}_{\mathrm{I}\,\mathrm{ext}}\right) \\ &= \mathbf{S}^{\mathrm{F}}\mathbf{f}^{\mathrm{mod}}_{\Gamma\,\mathrm{ext}} - \mathbf{S}^{\mathrm{F}}\left(\mathbf{S}^{\mathrm{S}}\right)^{-1}\mathbf{f}^{\mathrm{F}}_{\Gamma,i}\end{aligned} \tag{31}$$

with the modified external force term

$$\begin{aligned}\mathbf{f}^{\mathrm{mod}}_{\Gamma\,\mathrm{ext}} &= \left(\mathbf{S}^{\mathrm{F}}\right)^{-1}\mathbf{A}^{\mathrm{F}}_{\Gamma\mathrm{I}}\left(\mathbf{A}^{\mathrm{F}}_{\mathrm{II}}\right)^{-1}\mathbf{f}^{\mathrm{F}}_{\mathrm{I}\,\mathrm{ext}} \\ &\quad+\left(\mathbf{S}^{\mathrm{S}}\right)^{-1}\left(\mathbf{f}^{\mathrm{S}}_{\Gamma\,\mathrm{ext}} - \mathbf{A}^{\mathrm{S}}_{\Gamma\mathrm{I}}\left(\mathbf{A}^{\mathrm{S}}_{\mathrm{II}}\right)^{-1}\mathbf{f}^{\mathrm{S}}_{\mathrm{I}\,\mathrm{ext}}\right).\end{aligned} \tag{32}$$

Taking the relaxation into account the interface forces can be given by

$$\mathbf{f}^{\mathrm{F}}_{\Gamma,i+1} = \mathbf{f}^{\mathrm{F}}_{\Gamma,i} + \omega_i\mathbf{S}^{\mathrm{F}}\left(\mathbf{f}^{\mathrm{mod}}_{\Gamma\,\mathrm{ext}} - \left(\left(\mathbf{S}^{\mathrm{F}}\right)^{-1} + \left(\mathbf{S}^{\mathrm{S}}\right)^{-1}\right)\mathbf{f}^{\mathrm{F}}_{\Gamma,i}\right) \tag{33}$$

which turns out to be a nonstationary Richardson iteration. And again in analogue to [16] the residuum is

$$\mathbf{g}_i = \tilde{\mathbf{f}}^{\mathrm{F}}_{\Gamma,i+1} - \mathbf{f}^{\mathrm{F}}_{\Gamma,i}. \tag{34}$$

5.4 Discussion

Constraining the enclosed volume along with the solution of the structural equation introduces one additional scalar condition into the structural system of equations. This one condition seriously damages the bandwidth of the system matrix, it couples all displacements on the wet surface. Additionally, the positive definiteness of the matrix is lost. Thus, the approach is rather expensive from a numerical point of view. In order to meet this challenge one could use a staggered solution scheme for the enhanced structure equations as, e.g. in path-following approaches in static nonlinear structural mechanics. A similar situation can be found in dynamic contact problems, too, and one could also adopt approaches from this field.

In the present case, the additional costs pertain obviously to the structural part only. And because the fluid solution costs are dominating in most FSI calculations the proposed algorithm presents a viable approach for many FSI simulations which require Dirichlet constraints on all fluid boundaries.

6 Alternative solution approaches

6.1 Neumann–Dirichlet partitioning

Alternatively to finding remedies to the dilemma the Dirichlet–Neumann partitioning suffers from one can change the partitioning itself. The natural choice for the problem under consideration, that is conveniently close to the original algorithm, is to reverse the exchange of boundary information between the fields.

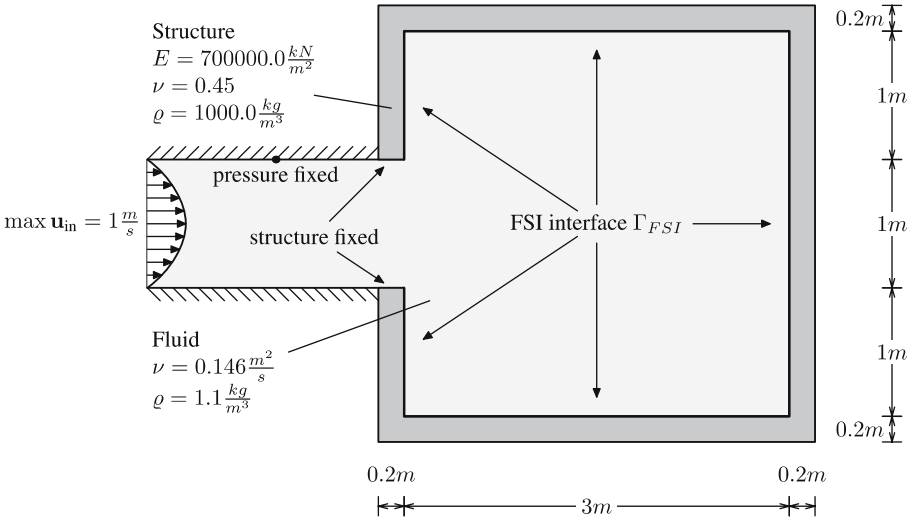

Fig. 2 A simple "balloon problem". The structure is *dark gray*. The inner area is filled with fluid

The resulting coupling algorithm might be called 'Neumann–Dirichlet partitioning' because the fluid domain acts as Neumann partition that is loaded with interface forces $\mathbf{f}_\Gamma$ from the structure. In return the fluid prescribes interface displacements $\mathbf{d}_\Gamma$ on the structure. This way the algorithm from Sect. 3.2 can be applied, only with the fields exchanged. With the abbreviation introduced in Eq. (13) the coupling algorithm reads:

1. Solve the structure dynamic equation with prescribed displacements $\mathbf{d}^{\text{F}}_{\Gamma,i}$.

$$\mathbf{A}^{\text{S}}_{\text{II}}\mathbf{d}^{\text{S}}_{\text{I},i+1} = \mathbf{f}^{\text{S}}_{\text{I ext}} - \mathbf{A}^{\text{S}}_{\text{I}\Gamma}\mathbf{d}^{\text{F}}_{\Gamma,i} \tag{35}$$

2. Calculate the reaction forces at the interface Γ_{FSI}

$$\mathbf{f}^{\text{S}}_{\Gamma,i+1} = \mathbf{A}^{\text{S}}_{\Gamma\text{I}}\mathbf{d}^{\text{S}}_{\text{I},i+1} + \mathbf{A}^{\text{S}}_{\Gamma\Gamma}\mathbf{d}^{\text{F}}_{\Gamma,i} \tag{36}$$

3. Solve the Navier–Stokes equation together with the mesh equation loaded with the interface forces $\mathbf{f}^{\text{S}}_{\Gamma,i+1}$ from the structure. This way fluid velocities, pressures, and interface displacements $\tilde{\mathbf{d}}^{\text{F}}_{\Gamma,i+1}$ are calculated.

$$\begin{bmatrix} \mathbf{A}^{\text{F}}_{\Gamma\Gamma} & \mathbf{A}^{\text{F}}_{\Gamma\text{I}} \\ \mathbf{A}^{\text{F}}_{\text{I}\Gamma} & \mathbf{A}^{\text{F}}_{\text{II}} \end{bmatrix} \begin{bmatrix} \tilde{\mathbf{u}}^{\text{F}}_{\Gamma,i+1} \\ \mathbf{u}^{\text{F}}_{\text{I},i+1} \end{bmatrix} = \begin{bmatrix} \mathbf{f}^{\text{F}}_{\Gamma\,\text{ext}} - \mathbf{f}^{\text{S}}_{\Gamma,i+1} \\ \mathbf{f}^{\text{F}}_{\text{I ext}} \end{bmatrix} \tag{37}$$

   Stop if the interface displacements changes are small enough.

4. Relax interface displacements.

$$\mathbf{d}^{\text{F}}_{\Gamma,i+1} = \omega_i \tilde{\mathbf{d}}^{\text{F}}_{\Gamma,i+1} + (1-\omega_i)\mathbf{d}^{\text{F}}_{\Gamma,i} \tag{38}$$

   And resume with step 1.

The coupling algorithm requires the fluid solver to solve the Navier–Stokes equation along with the mesh deformation algorithm, at least along the FSI interface. The increased coupling of the solvers is the algorithmic equivalent to the enhanced pressure coupling that was discussed in Sect. 5, yet the separation of the fluid and the structure solver is still preserved.

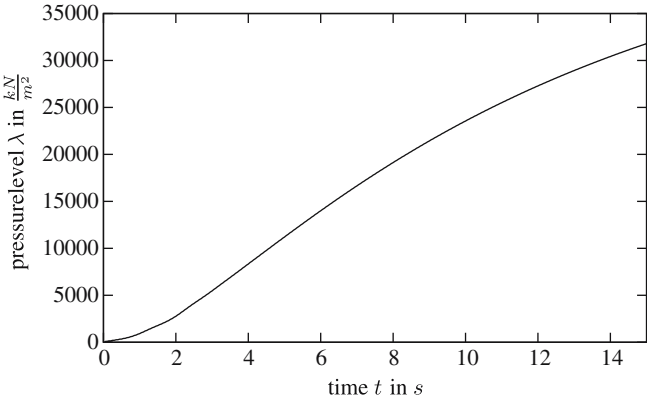

Fig. 3 The Lagrangian multiplier λ defines the pressure level of the fluid

Fluid domains that calculate their own deformation are known from free surface algorithms. Indeed, the fluid solver that is required here is a free surface solver with local Lagrangian conditions at the interface. To enhance the weak form of the Navier–Stokes equation with a mesh moving algorithm the mesh velocities $\mathbf{u}^{\text{G}}$ and the corresponding weighing function $\mathbf{w}$ are introduced. Both velocities are independent variables – the number of degrees of freedom increases – and the mesh movement has to be treated along with the fluid equation. In order to reduce computational costs, Wall et al. [27] couple the fluid and the mesh equations only in the region next to the FSI interface Ω_{FSI} and treat both equations separately in the internal region Ω_{int}.

In general, the mesh velocities at the mesh boundaries $\mathbf{u}^{\text{G}}_\Gamma$ are prescribed and thereby determine the velocities of the whole mesh. There are various mesh moving algorithms that can be employed, but for the current discussion the actual algorithm is of minor importance.

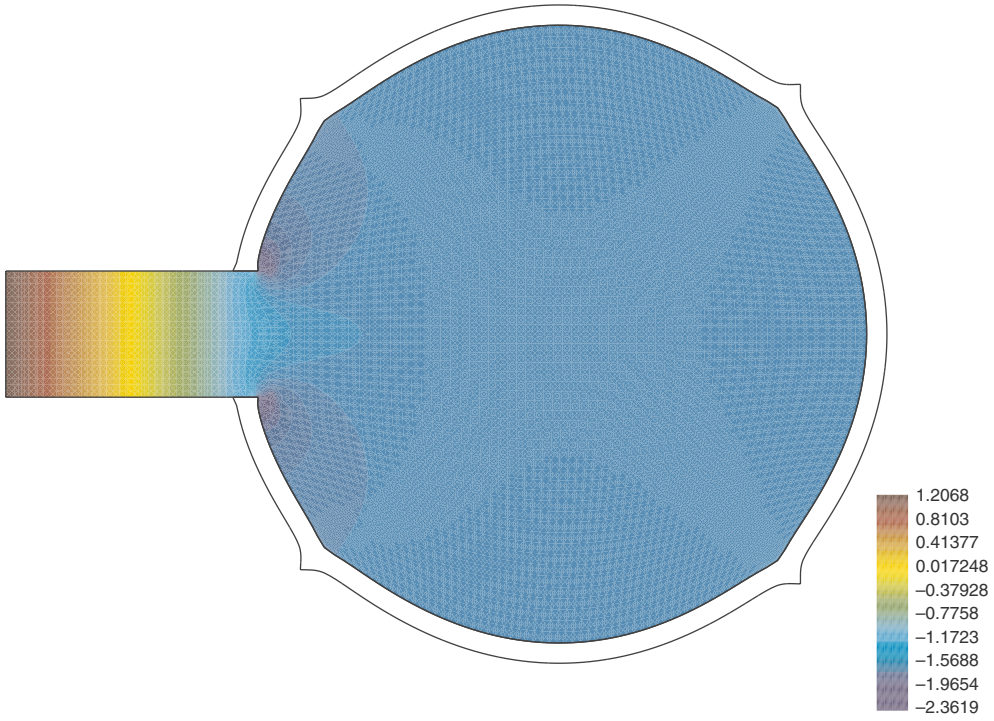

Fig. 4 Pressure p in kN/m^2 which adds to the constant pressure level λ in deformed balloon at time $t = 15s$

At the FSI interface Γ_{FSI} the fluid velocity $\mathbf{u}$ and the grid velocity $\mathbf{u}^{\text{G}}$ are equal. This equality is enforced by a constraint term.

$$\begin{aligned}&(\dot{\mathbf{u}}|_x, \mathbf{v}) + (2\nu\boldsymbol{\varepsilon}(\mathbf{u}), \boldsymbol{\varepsilon}(\mathbf{v})) - (\nabla p, \mathbf{v}) - (\nabla \cdot \mathbf{u}, q)\\ &\quad + (\mathbf{u} \cdot \nabla \mathbf{u}, \mathbf{v})_{\Omega_{\text{int}}} - \left(\mathbf{u}^{\text{G}} \cdot \nabla \mathbf{u}, \mathbf{v}\right)_{\Omega_{\text{int}}}\\ &\quad + (\mathbf{u} \cdot \nabla \mathbf{u}, \mathbf{v})_{\Omega_{\text{FSI}}} - \left(\mathbf{u}^{\text{G}} \cdot \nabla \mathbf{u}, \mathbf{v}\right)_{\Omega_{\text{FSI}}}\\ &\quad + \left(\mathbf{u} - \mathbf{u}^{\text{G}}, \boldsymbol{\lambda}\right)_{\Gamma_{\text{FSI}}} = (\mathbf{b}, \mathbf{v}) - \frac{1}{\varrho}\left(\mathbf{f}^{\text{S}}, \mathbf{v}\right)_{\Gamma_{\text{FSI}}}\end{aligned} \tag{39}$$

The boundary conditions for the free surface Navier–Stokes equation (39) are the same as those for the standard Navier–Stokes equation (6).The forces from the structure calculation $\mathbf{f}^{\text{S}}$ appear on the right-hand side of the fluid equation.

The free surface Navier–Stokes equation (39) has to be solved on an unknown domain. This introduces an additional difficulty, the linearization of Eq. (39) that is needed for the Newton iteration has to take the domain deformation into account. See [1, 7] for details on the required derivations.

The structure equation (1) does not need any modifications, only additional reaction forces have to be calculated and the relaxation procedure remains the same, too. The suggestions from [17] can be applied without modification, only the roles of the two fields are exchanged.

From a theoretical point of view there are no objections to the inverted Dirichlet–Neumann coupling. The algorithm works fine on a number of academic examples. But for real world problems unfortunately, the material parameters of any realistic FSI analysis cause unmanageable numerical difficulties. If there are stiff structures coupled with the fluid the structure's response to varying interface displacements will be much too sensitive, the gradient of the structure response will be much too steep for any numerical approach to find the equilibrium. This renders the algorithm unsuitable for the target applications. In addition, this approach obviously fails if incompressible structures are fully submerged.

6.2 Artificial (algorithmic) compressibility

Yet another line to attack the dilemma is to temporary remove the incompressibility of the fluid domain. That is the aim of the method of artificial compressibility that was first proposed in the 1960s [3]. The method was designed to be able to handle the numerical difficulties that stem from the fluid's incompressibility. It has been applied to steady and unsteady incompressible flows [20].

In the context of FSI analysis with fully Dirichlet bounded fluid domains, the method of artificial compressibility presents a way to avoid the incompressibility dilemma, to find the pressure level that satisfies the volume constraint from within the fluid and yet to reach the solution of the incompressible limit.

The method consists of enhancing the incompressibility constraint with a pressure derivation in pseudo-time that introduces compressibility.

$$\frac{1}{\beta}\frac{\partial p}{\partial \tau} + \nabla \cdot \mathbf{u} = 0, \tag{40}$$

where the pseudo-time τ is counted from the beginning of a time step. This term simplifies the numerical properties of

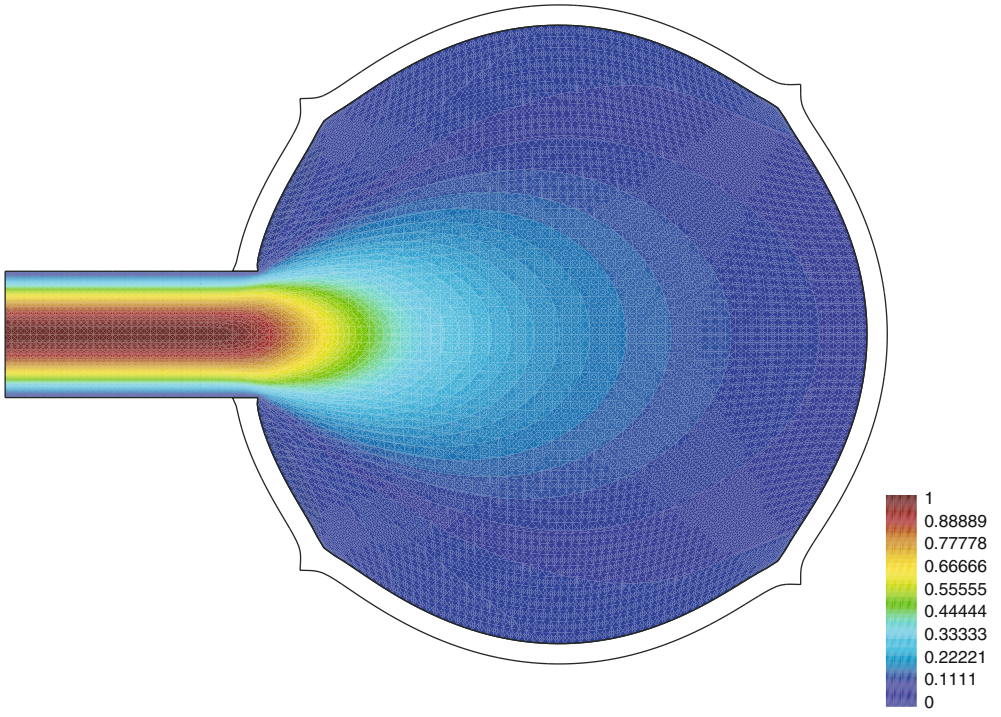

Fig. 5 Velocity $|\mathbf{u}|$ in m/s in deformed balloon at time $t = 15s$

the Navier–Stokes equation a lot, however an additional iteration in pseudo-time is needed within each time step in order to get rid of the artificially introduced compressibility.

$$\frac{1}{\beta}\frac{p_{i+1}^{n+1}}{\Delta\tau} + \nabla\cdot\mathbf{u} = \frac{1}{\beta}\frac{p_{i}^{n+1}}{\Delta\tau} \tag{41}$$

With this modification the algorithm from Sect. 3.2 has to be executed within each pseudo-time step. The resulting numerical procedure is expensive to say the least and because the incompressibility is only approximated the resulting pressure shows some instabilities.

To obtain an algorithm of practical relevance the additional pseudo-time iteration must be avoided. There are attempts to merge the pseudo-time iteration with the coupling iteration [19]. These attempts, however, have to converge two unknowns – the interface displacement and the fluid pressure – with just one iteration, something that can only be done if extra information is provided. The idea in [19] is to choose a suitable β such that the fluid pressure calculated by the pseudo-time iteration matches the overall elastic response of the structure. This idea is based on the assumption of a linear elastic structure, so that the structure's pressure response can be estimated on the fluid side. However, it remains unclear how to find an ersatz stiffness in complex cases and how the general nonlinear case should be treated. In essence all attempts to merge these two iterations require to know some part of the solution in advance.

In summary this artificial compressibility approach allows to find an approximation to the solution only in cases where an appropriate ersatz stiffness is known. An efficient algorithm has yet to be found, though.

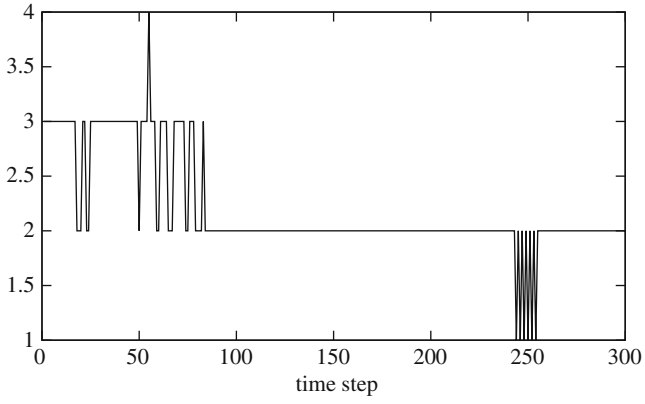

Fig. 6 Field iteration count of the simple balloon calculation

7 Numerical examples

All examples have been calculated by the modified Dirichlet–Neumann algorithm with volume constraint in the structural equation that is shown in Sect. 5.2.

7.1 Simple balloon-like problem

The purpose of the first example is to demonstrate the proposed algorithm with a largely varying enclosed area. The

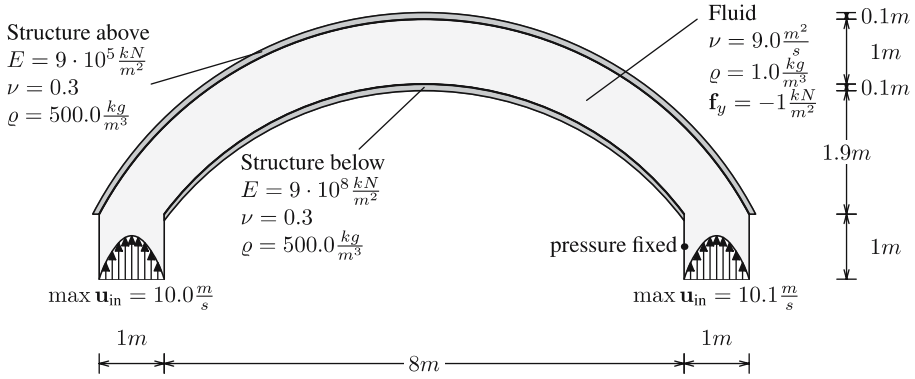

Fig. 7 A bended fluid domain with two inflow boundaries constraint by structures of different stiffness

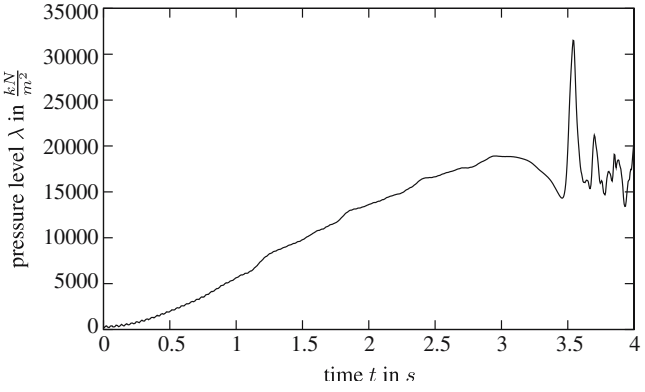

Fig. 8 Pressure level of the bended fluid domain

system is depicted in Fig. 2. It consists of a structure with neo-Hookean material that surrounds the fluid area fully but for the inflow boundary. The fluid velocities $\mathbf{u}_{\text{in}}$ are prescribed. The time step for the simulation is $\Delta t = 0.05s$ and the stepping curve $\sin(t/2s\pi)$ is applied for $t < 1s$.

To solve the problem, the algorithm from Sect. 5 with a volume constraint in the structure equation is used. During the coupling iteration the fluid pressure is set to 0 at the indicated point. The fluid's pressure level is therefore defined. The Lagrangian multiplier λ does not vanish and has to be added to the pressure calculated by the fluid to obtain the pressure that is in equilibrium with the structure. Figure 3 shows the increasing Lagrangian multiplier λ over time, that is the real fluid pressure at the point where for algorithmic reasons 0 is prescribed.

In this example the pressure variation in the fluid region, the pressure gradient, is very small compared to the pressure level that is needed to push the structure. It is therefore advisable to visualize the pressure gradient without the pressure level λ. As an example Fig. 4 shows the pressure gradient at time $t = 15s$ as calculated by the fluid solver. The corresponding velocity is shown in Fig. 5.

The effectivity of the proposed coupling algorithm is depicted by the number of field iterations needed per time step as shown in Fig. 6. The small number of iterations needed suggests that Aitken style relaxation of the interface forces is again a suitable approach.

7.2 Damped structural instability

A second example consists of a bended fluid domain that is surrounded by two thin structures with neo-Hookean material and different stiffness. The system is shown in Fig. 7. The structures are fixed at their short edges, the long edges are free, respectively, interacting with the fluid. At both inflow boundaries velocities are prescribed with the left one a little less than the right in order to avoid perfect symmetry. The fluid is loaded with the body force $\mathbf{f}_y = -1N/m^2$ in y direction. The simulation is carried out utilizing the augmented Dirichlet–Neumann algorithm and a uniform time step size $\Delta t = 0.005s$.

The constant inflow increases the fluid pressure so that first mainly the soft flexible structure above the fluid domain deforms to make room for the fluid. When a critical pressure value is reached the structure below the fluid collapses, however the instability is damped by the fluid volume constraint. That is why the deformation and the corresponding pressure decrease occur rather slowly. (Since this example is given just in order to demonstrate the augmented Dirichlet–Neumann approach, possible cavitation effects are not considered.) Afterward the system is in motion, the pressure varies rapidly in this phase. The pressure level development is depicted in Fig. 8.

Because the fluid pressure level is much larger than the pressure gradient variation there is again not much use in depicting the absolute pressure values. Instead Fig. 9 shows only the pressure gradient in the deformed configuration as calculated by the fluid solver. The pressure is fixed to 0 at the point indicated in Fig. 7. The negative pressures below that point are due to the body force $\mathbf{f}_y$. To obtain the real pressure the corresponding pressure level from Fig. 8 has to be added.

Figure 10 shows the corresponding absolute velocities. And to demonstrate the algorithm's effectivity Fig. 11 shows the number of field iterations needed in each time step.

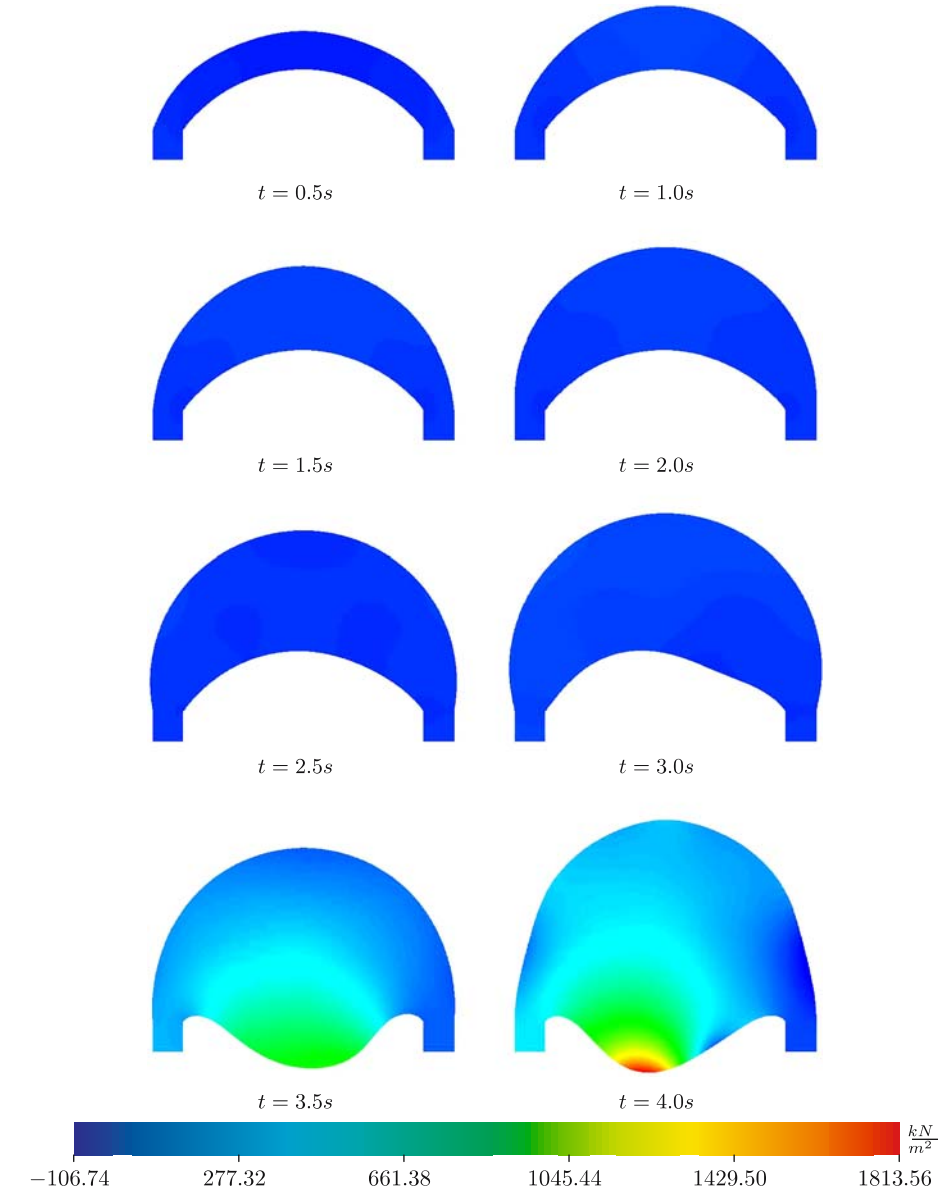

Fig. 9 Pressure p which adds to the constant pressure level λ. The structure part is not shown

8 Conclusion

An approach is presented which introduces a minor augmentation into the partitioned Dirichlet–Neumann algorithm for FSI problems which allows to solve problems where the fluid domain is entirely enclosed by Dirichlet boundaries. The incompressibility constraint of the fluid domain is added to the structural equations as a constraint yielding the pressure level information required to satisfy the volume constraint.

While – as in many other Lagrangian multiplier situations – introducing a numerically unfavorable equation which couples all degrees of freedom which belong to the wet surface Γ_{FSI} the augmentation regards the structural field only which frequently consumes the minor computation time of the overall algorithm. Thus, minimal additional effort is introduced to the overall coupled approach.

The proposed modification requires to directly transfer the structural displacement to the fluid field without relaxation. Thus in order to preserve the robustness properties of the method the force coupling information rather than the displacements are relaxed in accelerated strong coupling algorithms.

Numerical examples demonstrate the capability and efficiency of the augmented Dirichlet–Neumann algorithm.

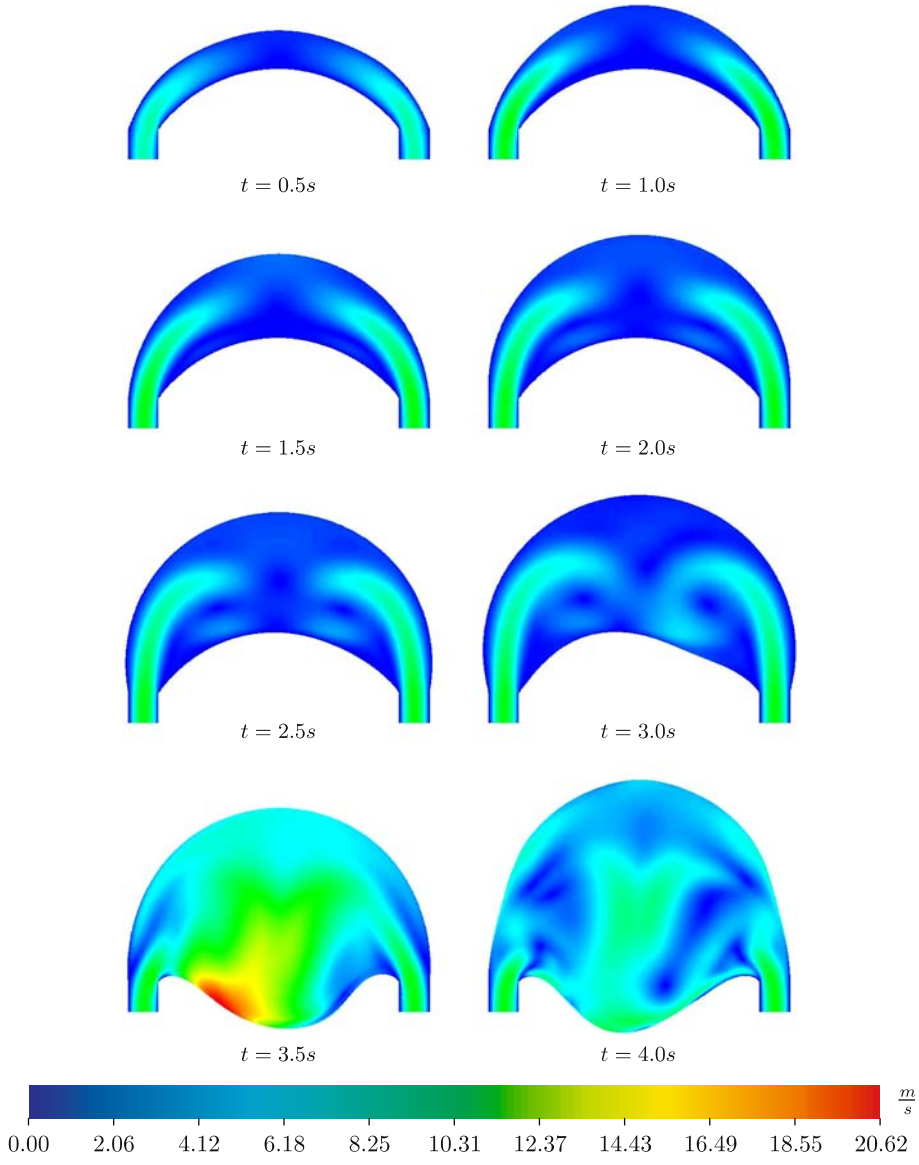

Fig. 10 Fluid velocity $|\mathbf{u}|$. The structure part is not shown

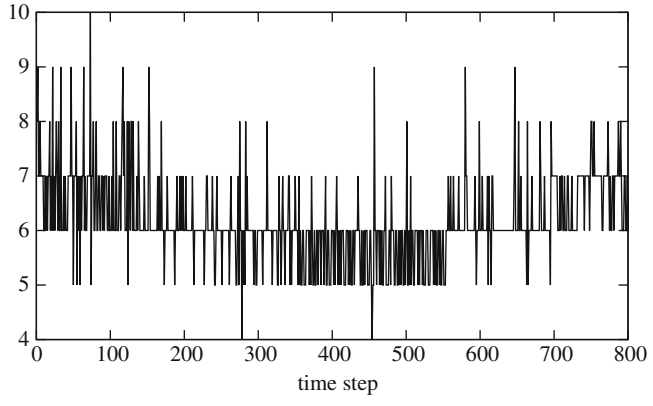

Fig. 11 Field iteration count of the bend fluid domain snap-through calculation with Aitken-style relaxation

References

1. Braess H, Wriggers P (2000) Arbitrary Lagrangian Eulerian finite element analysis of free surface flow. Comput Meth Appl Mech Eng 190:95–109
2. Causin P, Gerbeau J-F, Nobile F (2005) Added-mass effect in the design of partitioned algorithms for fluid–structure problems. Comput Meth Appl Mech Eng 194:4506–4527
3. Chorin AJ (1997) A numerical method for solving incompressible viscous flow problems. J Comput Phys 135:118–125
4. Chung J, Hulbert GM (1993) A time integration algorithm for structural dynamics with improved numerical dissipation; the generalized-α method. J Appl Math 60:371–375
5. Deparis S (2004) Numerical analysis of axisymmetric flows and methods for fluid–structure interaction arising in blood flow simulation. PhD thesis, EPFL
6. Deparis S, Discacciati M, Fourestey G, Quarteroni A (2006) Fluid–structure algorithms based on Steklov–Poincaré operators. Comput Meth Appl Mech Eng DOI 10.1016/j.cma.2005.09.029

7. Fernández MÁ, Moubachir M (2005) A Newton method using exact Jacobians for solving fluid–structure coupling. Comput Struct 83(2–3):127–142
8. Förster Ch, Wall WA, Ramm E (2006) Artificial added mass instabilities in sequential staggered coupling of nonlinear structures and incompressible flow, Preprint SFB 404, University of Stuttgart
9. Förster Ch, Wall WA, Ramm E (2006) On the geometric conservation law in transient flow calculations on deforming domains. Int J Numer Meth Fluids 50(12):1369–1379
10. Gerbeau J-F, Vidrascu M (2003) A quasi-Newton algorithm based on a reduced model for fluid–structure interaction problems in blood flows. Math Model and Numer Anal 37(4):631–647
11. Gerbeau J-F, Vidrascu M, Frey P (2005) Fluid–structure interaction in blood flows on geometries coming from medical imaging. Comput Struct 83:155–165
12. Heil M (2004) An efficient solver for the fully coupled solution of large-displacement fluid–structure interaction problems. Comput Meth Appl Mech Eng 193:1–23
13. Hübner B, Walhorn E, Dinkler D (2004) A monolithic approach to fluid–structure interaction using space–time finite elements. Comput Meth Appl Mech Eng 193:2087–2104
14. Le Tallec P, Mouro J (2001) Fluid structure interaction with large structural displacements. Comput Meth Appl Mech Eng 190:3039–3067
15. Matthies HG, Steindorf J (2003) Partitioned strong coupling algorithms for fluid–structure interaction. Comput Struct 81:805–812
16. Mok DP (2001) Partitionierte Lösungsansätze in der Strukturdynamik und der Fluid–Struktur-Interaktion. PhD thesis, Institut für Baustatik, Universität Stuttgart
17. Mok DP, Wall WA (2001) Partitioned analysis schemes for the transient interaction of incompressible flows and nonlinear flexible structures. In: Wall WA, Bletzinger K-U, Schweitzerhof K (eds) Trends in computational structural mechanics
18. Piperno S (1997) Explicit/implicit fluid/structure staggered procedures with a structural predictor and fluid subcycling for 2d inviscid aeroelastic simulations. Int J Numer Meth Fluids 25:1207–1226
19. Raback P, Ruokolainen J, Lyly M, Järvinen E (2001) Fluid–structure interaction boundary conditions by artificial compressibility. ECCOMAS Comp Fluid Dynamcs Conference 2001, Swansea, Wales, UK
20. Rogers SE (1995) A comparison of implicit schemes for the incompressible Navier–Stokes equations and artificial compressibility. AIAA J 33(11):2066–2072
21. Tezduyar TE (2004) Finite element methods for fluid dynamics with moving boundaries and interfaces. In: Stein E, De Borst R, Hughes TJR (eds) Encyclopedia of computational mechanics, vol 3, chapt 17. Wiley, New York
22. Tezduyar TE, Sathe S, Keedy R, Stein K (2004) Space–time techniques for finite element computation of flows with moving boundaries and interfaces. In: Proceedings of the III international congress on numerical methods in engineering and applied sciences, Monterrey, Mexico, January 2004
23. Tezduyar TE, Sathe S, Keedy R, Stein K (2006) Space–time finite element techniques for computation of fluid–structure interactions. Comp Meth Appl Mech Engng 195:2002–2027
24. Vierendeels J (2005) Implicit coupling of partitioned fluid-structure interaction solvers using a reduced order model. In: 35th AIAA fluid dynamics conference and exhibit. Toronto, Ontario, June 6–9 2005. AIAA
25. Wall WA (1999) Fluid–Struktur-Interaktion mit stabilisierten Finiten Elementen. PhD thesis, Institut für Baustatik, Universität Stuttgart
26. Wall WA, Mok DP, Ramm E (1999) Partitioned analysis approach of the transient coupled response of viscous fluids and flexible structures. In: Wunderlich W (ed), Solids, structures and coupled problems in engineering, proceedings of the European conference on computational mechanics ECCM '99, Munich
27. Wall WA, Genkinger S, Ramm E (2006) A strong coupling partitioned approach for fluid–structure interaction with free surfaces. Computers & Fluids, DOI 10.1016/j.comfluid.2005.08.007